Observation of Blueshifted Ultralong-Range Cs_2 Rydberg Molecules

J. Tallant,[1] S. T. Rittenhouse,[2,*] D. Booth,[1] H. R. Sadeghpour,[2,†] and J. P. Shaffer[1,‡]

[1]*Homer L. Dodge Department of Physics and Astronomy, The University of Oklahoma, 440 W. Brooks Street, Norman, Oklahoma 73019, USA*

[2]*ITAMP, Harvard-Smithsonian Center for Astrophysics, 60 Garden Street, Cambridge, Massachusetts 02138, USA*

(Received 22 May 2012; revised manuscript received 2 August 2012; published 23 October 2012)

We observe ultralong-range blueshifted Cs_2 molecular states near $ns_{1/2}$ Rydberg states in an optical dipole trap, where $31 \leq n \leq 34$. The accidental near degeneracy of $(n-4)l$ and ns Rydberg states for $l > 2$ in Cs, due to the small fractional ns quantum defect, leads to nonadiabatic coupling among these states, producing potential wells above the ns thresholds. Two important consequences of admixing high angular momentum states with ns states are the formation of large permanent dipole moments, ~15–100 Debye, and accessibility of these states via two-photon association. The observed states are in excellent agreement with theory.

DOI: 10.1103/PhysRevLett.109.173202 PACS numbers: 34.50.Cx, 32.80.Ee, 34.20.Cf

The observation of ultralong-range Rydberg molecules has piqued interest in few-body Rydberg interactions occurring in ultracold atomic gases [1–3]. The interaction for an exotic class of these systems, trilobite molecules, arises to first order from the zero-range pseudopotential scattering of a Rydberg electron from a ground state perturber. Part of the fascination originates from the prediction that these molecules can possess massive permanent electric dipole moments, ~1 kDebye [4]. Large dipole moments are expected when high electron angular momentum hydrogenic manifolds are involved in the electron-atom scattering. Ultracold Rydberg molecules formed by two-photon association into Rb(ns) states were expected only to have an induced dipole moment [1]. It was later demonstrated theoretically and experimentally [5] that due to the near integer quantum defect of Rb(ns), $\mu_s = 3.13$, nearly degenerate $(n-3)$ manifolds mixed highly localized trilobitelike states into the zeroth-order symmetric ns states at a level of 0.01%, giving them an observable permanent dipole moment, ~1 Debye.

We report the observation of ultralong-range trilobitelike Rydberg molecules formed in an ultracold gas of Cs in an optical dipole trap with large permanent electric dipole moments. The spectroscopic signature of these molecules is in excellent agreement with theoretical predictions and serves as a milepost for creating trilobite molecules with giant dipole moments. The unique features of these ultralong-range Rydberg molecules are threefold. First, these states are unexpectedly blueshifted with respect to the Cs(ns) thresholds. This feature results from the fact that the fractional part of the Cs(ns) quantum defect is small, $\mu_s = 4.05$, and $(n-4)l$, $l > 2$, "trilobite" manifolds become nearly degenerate and mix strongly with the ns states [5], inducing nonadiabatic avoided crossings of the ns-dominated Born-Oppenheimer (BO) potential energy curves. Second, the energetic proximity to the degenerate high-angular momentum hydrogenic states results in the molecular wave function having hydrogenic character at the 1% level. Therefore, large permanent electric dipole moments (15–100 Debye) are predicted. The large hydrogenic character of the wave function is promising for generating trilobite molecules with kD dipole moments. Third, the position of the Cs trilobite states depends sensitively on the location of the p-wave e^--Cs scattering resonance [6], and therefore the spectra serve as an indirect probe of the accuracy of the $^3P_1$ resonance position [7]. We find that a 10% shift of the scattering resonance position results in an 11% shift of the lowest bound vibrational level in the $M_J = \pm 1$ manifold in Fig. 1(a). This shift

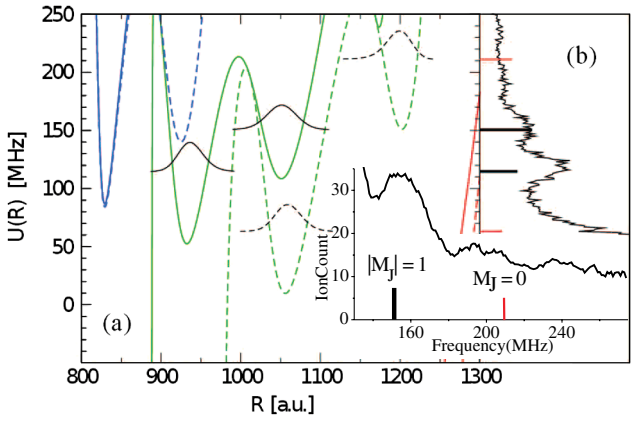

FIG. 1 (color online). (a) The $n = 31$ BO potential energy curves for $M_J = \pm 1$ (solid curves) and $M_J = 0$ (dashed curves) Cs_2 Rydberg molecules in the vicinity of the ns Rydberg threshold. Also shown are the low lying vibrational wave functions in the experimentally accessible region. The zero of energy is set to the appropriate $31s_{1/2}$ atomic Rydberg energy. (b) The experimentally observed spectra are shown in arbitrary units compared to the BO potentials. The line sticks give the positions of the predicted energies and relative transition strengths of the predissociating vibrational states. The two $M_J = \pm 1$ vibrational levels have calculated permanent dipole moments of 33.5 and 37.4 D, respectively. The inset is a blowup of the average of four spectral runs to show evidence for the $M_J = 0$ line.

($\approx$ 13 MHz) is larger than the measured half-width ac Stark shift. Unlike atoms in magnetic traps, both parallel and perpendicular projections of the magnetic quantum number (i.e., $M_J = 0, \pm 1$) of the triplet molecules [4,5] can be observed in an optical dipole trap.

In Fig. 1, we present the main result. The observed blueshifted Cs Rydberg molecular spectrum accurately correlates with the calculated vibrational lines for states near the Cs($31s$) threshold. Both $M_J = 0, \pm 1$ molecular symmetries are present. The blueshifted potential wells arise from the strong nonadiabatic BO coupling of the $31s$ state with the localized $27l$, $l > 2$, states. The binding energies are most easily defined with respect to the ns threshold as each BO potential has largely s character in the region where the spectroscopic resonances are observed. The molecular features are broadened with increasing energy from the $31s$ threshold. This can be understood to be the result of progressively larger permanent dipole moments, as the higher energy states have more high l character.

Relatively large densities and ultracold temperatures are required to efficiently create these molecules. The Cs molecules are photoassociated inside a crossed far off-resonance trap (FORT), which is loaded from a Cs vapor cell magneto-optical trap (MOT). The experimental setup has been described elsewhere [8]. The crossed FORT is prepared from a 10 W 1064 nm Yb fiber laser. The Yb laser beam is focused to a spot size ($1/e^2$) of 86 ± 1.1 μm. The crossed trapping region is slightly cigar shaped with a 2:1 aspect ratio. The beam paths are not interferometrically stabilized, so any effect of fringes is washed out over the course of the measurements. The FORT depth is $\sim$1.5 mK. The highest trap frequency is $2\pi \times 2.23$ kHz, and the lowest trap frequency is $2\pi \times 445$ Hz. The crossed FORT is loaded to a peak density of $\sim 2 \times 10^{13}$ cm^{-3}. To account for the combined ac Stark shifts of the ground and Rydberg states, the position of the Rydberg state was measured inside the MOT and compared to the position of the Rydberg state in the crossed FORT. The measured average ac Stark shift is 19 MHz.

The molecular states are excited by using a two-photon process. The first step is an infrared (IR) photon which is tuned 182 MHz red of the Cs $6p_{3/2}$ hyperfine manifold. The second photon is generated by a ring dye laser tuned near 512 nm. The infrared beam is sent through an acousto-optic modulator (AOM). The AOM diffraction order is carefully chosen to place ghost hyperfine peaks and peaks due to leakage light on the red side of the nearby Rydberg state. The output is collimated to a size of 1 mm^2 and has 5 mW of power. The green beam is also sent through an AOM. The output is focused onto the crossed region with a spot size of 44 μm and power of 70 mW. The two-photon linewidth of the excitation pulses was measured to be $<$3 MHz.

The green laser is scanned on the blue side of the $ns_{1/2}$ Rydberg states, while the IR laser remains locked 182 MHz below the Cs $6s_{1/2}(F = 3) \rightarrow 6p_{3/2}(F = 2)$ transition. An absorption spectrum is acquired by monitoring the number of ions produced as a function of green laser frequency. The excitation pulses begin 20 ms after the FORT has been loaded to let the uncaptured MOT atoms fall away. Each excitation pulse is 10 μs long and is immediately followed by an electric field pulse to project any positive ions onto a microchannel plate detector where they are counted. The excitation step repeats at 1.0 kHz and lasts 500 ms, at which time the green laser frequency is incremented by 1 MHz and the crossed FORT is reloaded. The atomic density decreases during the measurement cycle. The electric field used to extract the ions, 67 V cm^{-1}, is far below the ionization threshold of any Rydberg states in the experiment [9]. The FORT beam is used to photoionize any Rydberg atoms as well as the Rydberg atom constituents of the ultralong-range molecules. The ionization is not state selective in our experiment [8]. The signal from Rydberg atoms with the lasers on resonance is $>10^4$ times larger than the ultralong-range Rydberg molecular peaks observed. As many as six absorption spectra are averaged together with scaled frequencies to obtain a single experimental spectrum. Ions arriving at the molecular time of flight were not observed, suggesting a different decay mechanism than found in Ref. [1]. However, if the molecules gain >1 GHz of energy, they will be lost from the ionization region.

The absolute frequency of the IR beam is monitored with a saturated absorption setup. The light for the saturated absorption is shifted with AOMs such that the Cs $6s_{1/2}(F = 3) \rightarrow 6p_{3/2}(F = 3)$ transition is on resonance during the experiment. The saturated absorption spectrum determines the IR frequency within $\sim$3 MHz. To monitor the frequency of the green laser, a fraction of the laser output is combined with light from the IR laser to generate an electromagnetically induced transparency signal in a room-temperature Cs vapor cell. This arrangement produces up to six electromagnetically induced transparency resonances corresponding to different hyperfine states and detunings whose absolute frequency relations are known to provide spectroscopic markers.

The bonding of these types of Rydberg molecules derives from the frequent scattering of the highly excited Rydberg electron from the ground state atom perturber [4,10]. The relevant electron-ground state atom interaction is described within the zero-range Fermi pseudopotential approximation [11,12],

$$V_{e-a}(\mathbf{r}) = 2\pi A_s(k)\delta^{(3)}(\mathbf{r} - \mathbf{R}) + 6\pi A_p^3(k)\delta^{(3)}(\mathbf{r} - \mathbf{R})\overleftarrow{\nabla} \cdot \vec{\nabla}, \quad (1)$$

where A_s and A_p are the energy-dependent s- and p-wave scattering length, respectively, and $\mathbf{r}$ and $\mathbf{R}$ denote the positions of the electron and ground state atom relative to the Rydberg core, respectively. The BO potentials which

support the molecular predissociating states are found by diagonalizing the interaction of Eq. (1) in a basis of Rydberg electron nl orbitals [5,6]. Within the semiclassical picture the electron wave number k is related to the intermolecular distance R by $k = \sqrt{2(1/R - E_b)}$, where E_b is the binding energy of the isolated Rydberg atom. The energy-dependent scattering lengths are given by $A_s(k) = -\tan\delta_s/k$ and $A_p^3(k) = -\tan\delta_p/k^3$, where δ_l is the scattering phase shift for l-wave electron Cs scattering. Cs has relatively large spin-orbit interaction resulting in different ($J = 0$, 1, and 2) e^--Cs ^3P_J resonant scattering phase shifts. To account for this, we take the p-wave scattering to be

$$A_p^3 = \sum_{J=0}^{2} [C_{10,1M_J}^{JM_J}]^2 A_{p,J}^3, \tag{2}$$

where $C_{L_1M_1,L_2M_2}^{JM_J}$ is a Clebsch-Gordan coefficient coupling the bound e^- angular momenta (L_1M_1) to the scattering e^- angular momenta (L_2M_2). The different Clebsch-Gordan coefficients create different potentials for the $M_J = \pm 1$ and 0 cases. The p-wave scattering lengths are found by setting the $^3P_1$ resonance position to 8 meV [7] and the splitting of the $^3P_0$ and $^3P_2$ states to those of Ref. [13].

The resulting BO potentials near the ns Rydberg threshold are shown for $n = 31$–34 in Figs. 1 and 2(b)–2(d), respectively, for total angular momentum projection $M_J = \pm 1$ (solid curves) and 0 (dashed curves). Figure 2(a) shows the $n = 31$ BO potentials over a larger energy range correlating to atomic Rydberg thresholds in the vicinity of the Cs(31s) state. The near degeneracy of the $(n-4)l > 2$ manifolds with the ns series ensures that there are nonadiabatic couplings between the molecular potential energy curves of the same symmetry. Two important consequences of this interaction are the formation of potential wells capable of supporting bound states, blueshifted with respect to the ns Rydberg thresholds, and accessibility of these states via two-photon association. Figures 2(b)–2(d) also show several of the low lying vibrational wave functions within the experimentally accessible region. The

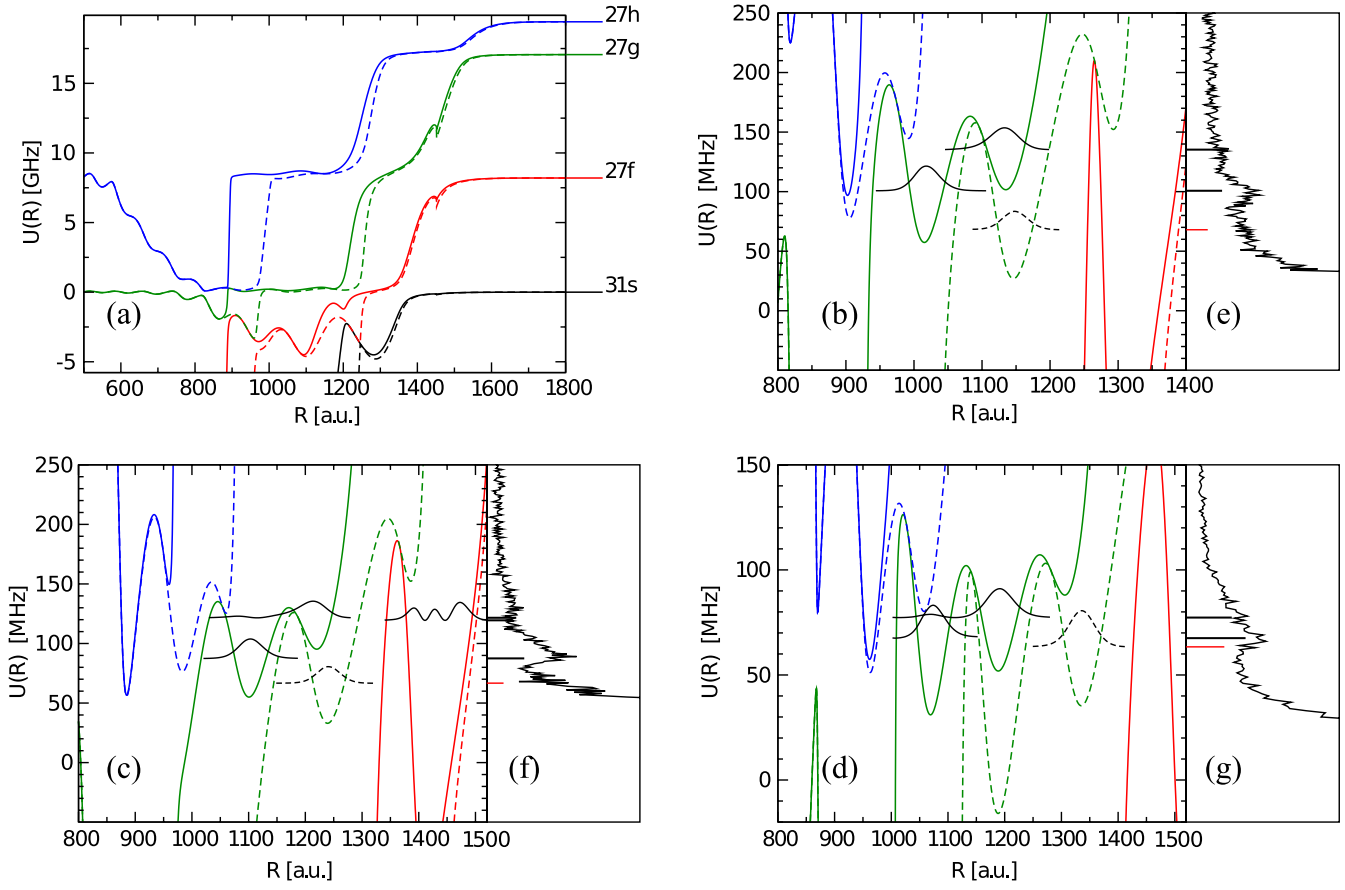

FIG. 2 (color online). (a) The BO potential energy curves for $M_J = \pm 1$ (solid curves) and $M_J = 0$ (dashed curves) correlating to atomic Rydberg thresholds in the vicinity of the Cs(31s) state. Note that the avoided crossings of BO potential energy curves result in blueshifted potential wells, capable of supporting localized vibrational states with significant s character. The $n = 32$–34 BO potential energy curves for $M_J = \pm 1$ (solid curves) and $M_J = 0$ (dashed curves) are displayed in (b)–(d) and the corresponding observed spectra are shown in (e)–(g), respectively. For detailed description of the features, see the caption for Fig. 1. The zero on the energy axis refers to the corresponding Cs(ns) threshold.

averaged experimental data near the $ns_{1/2}$ Rydberg states for $n = 31$–34 are compared with the theoretical predictions and show excellent agreement. All of the molecular states have spatial angular momentum projection $M_L = 0$ [4,6]; i.e., all of the states are $^3\Sigma$ molecules. While there exist BO potential energy curves corresponding to the $^3\Pi$ symmetry, they do not couple to the molecular states considered here [6]. Because the BO potentials near the ns thresholds are sensitive to the position of the $^3P_1$ resonance, the agreement between theory and experiment can be used as an indirect probe of the accuracy of the resonance position [7]. Most of the observed states correspond to the $M_J = \pm 1$ projections of the electronic angular momentum, but, because these states are photoassociated in a FORT, we are sensitive to the $M_J = 0$ projection as well. In all the spectra, we observe features which we tentatively assign to vibrational levels in the $M_J = 0$ potential energy curves. The position of the $M_J = 0$ vibrational states are sensitive to the position of the $^3P_0$ electron-atom resonance and not to the $^3P_1$ resonance position. As a result, these vibrational states could be better fit by adjusting the ^3P_J splitting rather than using the theoretical values of Ref. [13].

The molecules also experience an ac Stark shift in the FORT. As the molecular states consist of single Rydberg excitations, and the ac Stark shift of a Rydberg atom is only weakly dependent on the Rydberg state [9,14], we expect the Rydberg molecular states to exhibit the same shift and inhomogeneous broadening as the atomic transition. This hypothesis is corroborated by the fact that the observed data shifted by the measured atomic ac Stark shift, 19 MHz, are in good agreement with theory. The experimental widths of the most prominent states seen in Figs. 2(e)–2(g) are ~20 MHz, far larger than that expected from the atomic Rydberg linewidth, ~100 kHz [15] and that observed for the Cs Rydberg atoms, ~11 MHz. The additional broadening is likely due to the existence of large dipole moments for the Rydberg molecules, ~30 D. We expect small stray electric fields (on the order of 100 mV cm^{-1}) coupled to the large molecular dipoles to produce broadening in the range of 4–10 MHz. This estimate was made by approximating the molecule as a rigid rotor with the equilibrium distance set by the minimum of the outermost potential well and taking the maximum rotational level as determined by the temperature of the trap [16]. Each rotational state is broadened by the ac Stark effect, resulting in an overall linewidth of ~17–20 MHz. The strength of the dipole moments increases with increasing energy above the Cs(ns) thresholds, as the molecular states progressively retain less s-wave character. The observed molecular spectra in Figs. 1(b) and 2(e)–2(g) become progressively broadened with energy, lending further support to our assertion.

A molecule with a dipole moment of ~35 D should exhibit a dramatic linear Stark effect. To investigate this, small background electric fields were applied during excitation of the two $M_J = \pm 1$ molecular states near $n = 31$. Surprisingly, even electric fields below 100 mV cm^{-1} cause changes in the observed spectrum. A linear Stark effect is not observed. Rather, the observed peaks broaden and slightly shift to the blue (~ 10 MHz) before the bluest peak disappears completely. The additional broadening of the lines decreases their amplitude and complicates the measurement. The effect is different for each of the observed molecular states, which is to be expected based on their different potential minima. Our observations cannot be simply described as a linear Stark shift, because the potentials supporting the bound states are changing appreciably with the applied field. This is expected to be different than the Rb case [5], because the molecular states here have significant mixing with the degenerate hydrogenic manifold and are the result of avoided crossings. As a consequence, the electric field dependence is sufficiently complicated to prevent a full analysis in this Letter.

In summary, we have observed Cs "trilobitelike" Rydberg molecules in a crossed optical dipole trap and found the spectrum to be in excellent agreement with theory. The agreement with theory provides an experimental probe for the position of the p-wave resonance [7]. We present evidence for the observation of both $M_J = 0$ and $M_J = \pm 1$ states. The molecular states studied have significant highly localized trilobitelike electronic character. The additional line broadening observed is believed to arise from the large permanent electric dipole moment. We measured large changes in the spectrum by applying small electric fields, suggestive of both large permanent electric dipole moments and structural changes to the states, consistent with theory. In contrast with Rb, a large signal for the Cs_2^+ molecular ion is not observed, suggesting a different decay mechanism. The discovery of spectroscopically accessible Cs trilobite states opens another window into these exotic molecules. It may be possible to use these states to create ion pair states.

The authors thank C. H. Greene, T. Pfau, and L. Marcassa for helpful discussions. H. R. S. and S. T. R. acknowledge support through an NSF grant to ITAMP at Harvard University and the Smithsonian Astrophysical Observatory. The experiment was supported by the NSF (PHY-0855324 and PHY-1205392).

*Present address: Department of Physics and Astronomy, Western Washington University, Bellingham, WA 98225-9164, USA.
†hsadeghpour@cfa.harvard.edu
‡shaffer@nhn.ou.edu

[1] V. Bendowsky, B. Butscher, J. Nipper, J. P. Shaffer, R. Löw, and T. Pfau, Nature (London) **458**, 1005 (2009).
[2] K. R. Overstreet, A. Schwettmann, J. Tallant, D. Booth, and J. P. Shaffer, Nat. Phys. **5**, 581 (2009).

[3] V. Bendkowsky, B. Butscher, J. Nipper, J. B. Balewski, J. P. Shaffer, R. Löw, T. Pfau, W. Li, J. Stanojevic, T. Pohl, and J. M. Rost, Phys. Rev. Lett. **105**, 163201 (2010).
[4] C. H. Greene, A. S. Dickinson, and H. R. Sadeghpour, Phys. Rev. Lett. **85**, 2458 (2000).
[5] W. Li, T. Pohl, J. M. Rost, S. T. Rittenhouse, H. R. Sadeghpour, J. Nipper, B. Butscher, J. B. Balewski, V. Bendkowsky, R. Löw, and T. Pfau, Science **334**, 1110 (2011).
[6] A. A. Khuskivadze, M. I. Chibisov, and I. I. Fabrikant, Phys. Rev. A **66**, 042709 (2002).
[7] M. Scheer, J. Thøgersen, R. C. Bilodeau, C. A. Brodie, H. K. Haugen, H. H. Andersen, P. Kristensen, and T. Andersen, Phys. Rev. Lett. **80**, 684 (1998).
[8] J. Tallant, D. Booth, and J. P. Shaffer, Phys. Rev. A **82**, 063406 (2010).
[9] T. F. Gallagher, *Rydberg Atoms* (Cambridge University Press, Cambridge, England, 1994), 1st ed..
[10] C. Bahrim, U. Thumm, and I. I. Fabrikant, J. Phys. B **34**, L195 (2001).
[11] E. Fermi, Nuovo Cimento **11**, 157 (1934).
[12] A. Omont, J. Phys. (Paris) **38**, 1343 (1977).
[13] U. Thumm and D. W. Norcross, Phys. Rev. Lett. **67**, 3495 (1991).
[14] K. C. Younge, B. Knuffman, S. E. Anderson, and G. Raithel, Phys. Rev. Lett. **104**, 173001 (2010).
[15] B. Butscher, J. Nipper, J. B. Balewski, L. Kukota, V. Bendowsky, R. Löw, and T. Pfau, Nat. Phys. **6**, 970 (2010).
[16] A. Schwettmann, J. Franklin, K. Overstreet, and J. P. Shaffer, J. Chem. Phys. **123**, 194305 (2005).